RJC

RASĀYAN *J. Chem.*
Vol. 14 | No. 1 |493-509| January - March | 2021
ISSN: 0974-1496 | e-ISSN: 0976-0083 | CODEN: RJCABP
http://www.rasayanjournal.com
http://www.rasayanjournal.co.in

SYNTHESIS, *In-vitro* ANTIMICROBIAL, *In-silico* ADMET ANALYSIS AND DNA INTERACTION OF *N*-(8-HYDROXYQUINOLIN-5-YL)-4-METHYLBENZENESULFONAMIDE AND ITS METAL COMPLEXES: A COMBINED SPECTROSCOPY AND MOLECULAR DOCKING STUDIES

Ruby Kharwar and Ritu B. Dixit✉
Ashok and Rita Patel Institute of Integrated Study and Research in Biotechnology and Allied Sciences (ARIBAS), New Vallabh Vidyanagar-388121
✉Corresponding Author: ritsdixit@yahoo.co.in

ABSTRACT

Here we report the synthesis of *N*-(8-hydroxyquinolin-5-yl)-4-methylbenzenesulfonamide (8HQMBS) ligand and its metal (M(II)) complexes, where M = Mn(II), Fe(II), Co(II), Ni(II), Cu(II) & Zn(II) in 2:1 molar ratio. The synthesis was investigated by the study of physicochemical properties, elemental analysis, FT-IR, Mass, NMR, TGA, UV-Vis absorption spectroscopy, and magnetic susceptibility. Octahedral geometry of metal complexes was proposed based on the aforementioned analysis. *In vitro,* antibacterial and antifungal screening showed enhanced activity of ligand upon metal complexation. Complexes-DNA interaction was investigated and the results indicated that the complexes could strongly bind to CT-DNA by intercalation mechanism. *In silico* ADMET study revealed good drug-likeness characteristics of the compounds. Finally, a comparative molecular docking study with the bacterial proteins and a DNA helix was performed to offer better insight into the binding mechanism and critical interactions in their active pockets. The docking results confirmed the spectroscopic results.

Keywords: 8-Hydroxyquinoline, Sulfonamide, Antimicrobial, Molecular Docking, Pharmacokinetics, Toxicity
RASĀYAN *J. Chem.*, Vol. 14, No.1, 2021

INTRODUCTION

The resistance of the tumour to drugs is one of the major problems in cancer treatment.[1] Cisplatin and its derivatives are still used to treat cancer. However, they have several clinical disadvantages due to their restricted applicability, acquired tumour cell resistance and severe side effects such as nephrotoxicity and neurotoxicity.[2] Therefore, with the expectation of discovering a cheap metal complex with fewer side effects, low-cost and enhanced therapeutic values, a variety of metal-based drugs are being synthesized and studied.[3] The primary target of the anticancer drug is DNA.[4] The interaction between the drug and DNA could damage the cancer cell DNA, block their cell division and further result in cell death.[5] Metal complexes binding to DNA depends upon the geometry of compound in coordination,[6] and are of three types: (i) covalent binding DNA-alkylators or with Lewis acid metal ions, such as clinical use of platinum in various anticancer drugs[7] (ii) major or minor grooves binding[8] and (iii) intercalation.[9] The intercalation mode is the most significant of these interactions as it explicitly includes π–π interaction of the small molecules' planar aromatic part with the stacked aromatic planes of the nitrogen bases.[10] So, the search for drugs that shows intercalative binding mode has become the research area of interest for the past several decades.[11]

8-Hydroxyquinoline (8HQ) is considered a privileged structure for the design of new candidates for drugs. 8HQ derivatives have been studied for wide-ranging biological applications like metal chelators for neuroprotection, metalloproteins chelators, anticancer, antibacterial, antifungal, anti-HIV, antileishmanial, antischistosomal agent.[12] Some of the key disadvantages are linked to absorption, distribution, metabolism, excretion, and toxicity of 8HQs as drugs.[13] To overcome these disadvantages, 8HQ has been conjugated with other biologically active scaffolds to produce a molecule with enhanced efficacy and low toxicity.[14] The phenolate oxygen and pyridyl nitrogen atoms of 8-hydroxyquinoline moiety serve as the

http://dx.doi.org/10.31788/ RJC.2021.1415922

metal-binding sites for further complexation with bivalent transition metal ions such as Mn(II), Fe(II), Co(II), Ni(II), Cu(II) and Zn(II) etc. Metal complexes of 8HQ derivatives have been reported to be active against bacteria, as antiamoebic, antileishmanial, antimalarial, anticancer and antifungal.[15] Therefore, in the present study, 8HQ has been taken as a base moiety for further complexation with metal (II) salts. Sulfonamides are drugs of proven therapeutic importance and are used against a wide bacterial spectrum. But, many of the bacterial strains have developed resistance towards sulfa drugs.[16] However, the use of sulfa drugs has been extended by giving them as combination drugs in the treatment of cancer, malaria, leprosy and tuberculosis.[17] Nowadays sulfonamides are added to another biologically active scaffold to produce hybrid molecules. Compared to the multi-component drugs, hybrid compounds are more effective because of the risk of drug-drug interactions and their adverse effects are less likely to occur.[18] And this is how the use of sulfa drugs has been increased to treat diseases like diabetes, psychosis, malaria and tuberculosis.[19,20]

Our interest in coordination chemistry compelled us to synthesize sulfonamide derivative of 8-hydroxyquinoline and its metal complexes whose coordination chemistry is less developed in the literature. The synthesized molecules were tested for their antimicrobial properties and further ligand/complex-DNA binding studies were also performed. *In silico* antibacterial and DNA binding mode had been investigated to strengthen the results obtained *in vitro* and to give a detailed insight into ligand-protein/DNA interaction. Besides, all the synthesized compounds have been subjected to *in silico* ADMET parameter evaluation which is a required study to consider the synthesized molecules as a drug candidate. *In silico* ADMET analysis is the most effective technique for the pharmaceutical industry to predict the molecular properties of absorption, distribution, metabolism, excretion and toxicity behaviour while designing and developing a lead compound.[21]

EXPERIMENTAL

Chemicals and Reagents

For this study, all the chemicals and reagents used were of analytical grade and the highest purity available. They include 4-toluenesulfonyl chloride (Sigma-Aldrich), 5-amino-8-hydroxyquinoline dihydrochloride salt (Sigma-Aldrich), $MnCl_2.2H_2O$ (Hi-Media), $FeCl_2.6H_2O$ (Sigma-Aldrich), $NiCl_2.6H_2O$ (Hi-Media), $CoCl_2.6H_2O$ (Hi-Media), $CuCl_2.2H_2O$ (Hi-Media), $ZnCl_2.2H_2O$ (Sigma-Aldrich), NaOH (Sigma-Aldrich), CT-DNA (Hi-Media). Organic solvents used included absolute ethyl alcohol, acetonitrile, methanol and dimethyl sulfoxide (DMSO) were also obtained from Sigma-Aldrich. For all other preparations, double distilled water was used.

Instrumentation

The reaction and purity of the synthesized compounds were checked by TLC on silica gel F254 thin-layer chromatographic plates, size 20 × 20 cm, purchased from Merck (India) Limited. Melting points of compounds was checked by the open capillary method and were uncorrected. C, H, N, S analyzer of Perkin Elmer (the U.S.A, 2400 Series II) was used for the elemental analysis. Infrared spectra (FT-IR) were recorded in KBr pellets on the Perkin Elmer spectrum GX spectrophotometer instrument in the range 4000–400 cm^{-1}. The mass spectrum was recorded on a Shimadzu LC-MS 2010 eV mass spectrophotometer in DMSO. ^1H NMR and ^{13}C NMR were recorded on Bruker (400 MHz) instrument using TMS as an internal reference standard and DMSO d_6 as a solvent. UV-160Aspectrophotometer, Shimadzu, Kyoto (Japan) was used to record the electronic spectra of compounds. Using mercury tetrathiocyanato-cobaltate(II) as the calibrant ($\chi_g = 1644 \times 10^{-6}$ cgs units at 20 °C) at room temperature, the magnetic moments were determined by Gouy's method by using citizen balance. On a model (Mettler-Toledo) thermogravimetry analyzer, thermogravimetric analyses were performed at a heating rate of 10 °C min^{-1} in air. After decomposing the organic matter in mixing $HClO_4$, H_2SO_4 and HNO_3 (1: 1.5: 2.5), the metal content of the complexes was analyzed with EDTA titration.

Synthesis of *N*-(8-hydroxyquinolin-5-yl)-4-methylbenzenesulfonamide (8HQMBS)

4-Toluenesulfonyl chloride (0.75 mmol) was added dropwise to the solution of 5-amino-8-hydroxyquinoline dihydrochloride (0.70 mmol) in dry pyridine at 0-5 °C. The solution was stirred for 4 h

at 0-5 °C while, the reaction was monitored by TLC. The dark brown mixture was adjusted to pH 6 to obtain precipitates. The dark brown solid (8HQMBS) so formed, was collected by filtration, washed with double distilled water, chloroform, ethyl acetate and dried in vacuo.[22]

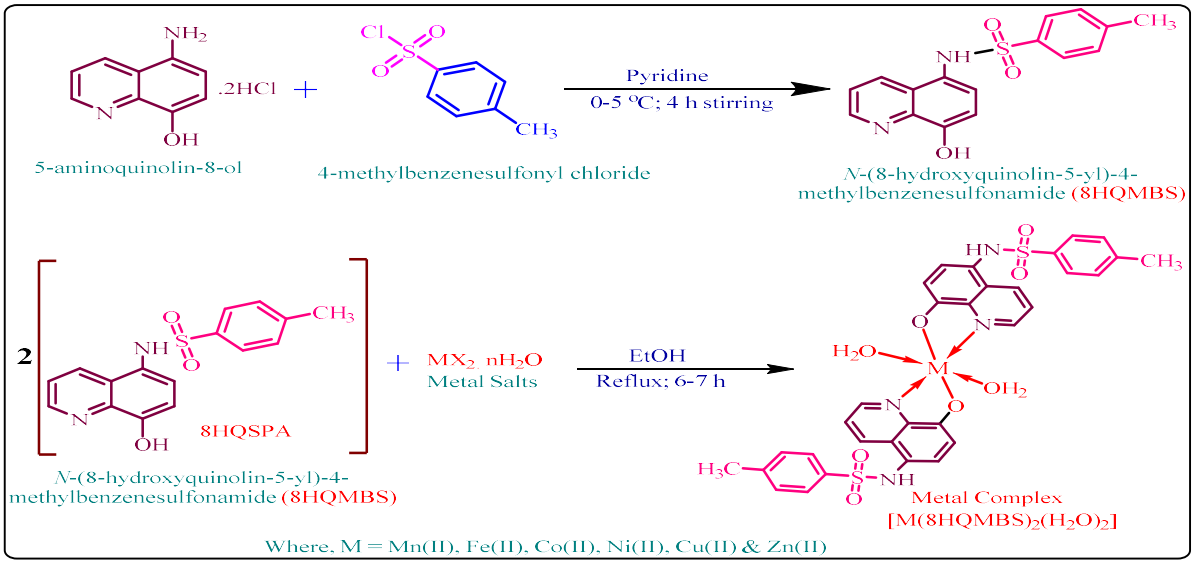

Scheme-1: Reaction Scheme to Synthesize 8HQMBS Ligand and its Metal Complexes

Synthesis of Metal Complexes of 8HQMBS Ligand

The entitled series of metal complexes were synthesized by complexation of before synthesized *N*-(8-hydroxyquinolin-5-yl)-4-methylbenzenesulfonamide (8HQMBS) ligand with various transition metal salts in presence of ethanol at refluxing temperature. To the warm solution of 8HQMBS, transition metal salts (chloride) were added dropwise in the stoichiometric ratio (2:1) respectively. The pH of the solution was adjusted to ~8.5 with 10% NaOH and the resultant mixture was allowed to reflux for 6-7 h till solvent reduces to a smaller volume and centrifuged. The solid residue produced was then filtered off, washed with distilled water, hot ethanol, acetonitrile, and dried in vacuum desiccators over calcium chloride. The resultant yield was calculated.[23] The formula of metal complexes are $M(II)(8HQMBS)_2(H_2O)_2$ where M(II) is Mn(II), Fe(II), Co(II), Ni(II), Cu(II), and Zn(II). The synthesis procedure is shown in Scheme-1.

Antibacterial and Antifungal Activity

In vitro antimicrobial screening against gram-positive bacteria (*S. aureus* (MTCC-96), *B. subtilis* (MTCC 441)), gram-negative bacteria (*E. coli* (MTCC 443), *P. aeruginosa* (MTCC-441)) and two fungi (*A. niger* (MTCC-282), *A. flavus* (NRRL- 21882) was carried out for all the synthesized compounds using broth microdilution minimum inhibitory concentration (MIC) method (NCCLS, 2002)).[24] As a nutrient medium, Mueller–Hinton Broth was used to grow and dilute the suspension for bacteria, likewise, for fungal nutrition, Sabouraud Dextrose Broth was used. A standard drug-like ampicillin and chloramphenicol for antibacterial and griseofulvin and nystatin for antifungal were used in screening.

Inoculums Preparation

Initially, the growth of bacterial strains was done by inoculating them overnight in Mueller–Hinton agar. The bacterial colonies were suspended in saline and its concentration was standardized by turbidimetric comparison to the McFarland norm (approximately 108 CFU/mL) and calibrated to 108 CFU/mL. Similarly, for fungi, nutrient media was prepared in sabouraud dextrose broth and further standardization of inoculum was done.

Drug Solutions Preparation

By first dissolving in DMSO, a desirable concentration of tested compounds and reference drugs was obtained, and further dilution was performed using the respective culture medium. The stock solutions

were prepared by diluting compound and standard drugs having 2,000 µg/mL concentrations. Primary screening for all synthesized compounds against all microbial strains was carried out by diluting stock solutions up to 1,000, 500, and 250 µg/mL for MIC determination. For secondary screening, compounds that showed positive results in primary screening were taken and tested at a lower concentration value.[25]

DNA Binding Studies

This study was carried out in the following ways:

Hydrodynamic Measurement (Viscosity Measurement)

Viscosity measurements were performed using a thermometric bath with the Ubbelohde viscometer held at a constant temperature. To decrease the complications resulting from its flexibility, calf thymus DNA (CT-DNA) was dissolved into phosphate buffer (Na_2HPO_4/NaH_2PO_4, pH 7.2). The DNA concentration was set at 200 µM in phosphate buffer and the flow time was measured using a digital stopwatch. Three measurements were taken and their mean value was used to test samples viscosity (η). Relative specific viscosity values $(\eta/\eta_0)^{1/3}$ were plotted against [DNA]/[complex][26] where η is the specific viscosity contributions of DNA in the presence of the complex and η_0 is the specific viscosity contribution of DNA in the absence of complex.

UV-Visible Absorption Titration

UV visible spectra were studied in the absence and presence of CT-DNA at a constant concentration of 8HQMBS and its metal complexes (10 µM) in phosphate buffer (pH 7.2). For this study, a fixed amount (10 µl) of 8HQMBS ligand and its metal complexes and a varying proportion (0, 4, 8 and 12 µl) of DNA solution was added in the phosphate buffer by maintaining the pH of the solution at 7.2. After incubation of 1 h, the spectra were recorded.[27]

DNA Binding through Gel Electrophoresis

0.8% agarose gel was prepared. 10 µl of the sample was loaded with 10 µl of bromophenol blue tracking dye. The electrophoresis was performed under TBE buffer system for 40 minutes at a constant voltage of 50 V.[28] 3 µl ethidium bromide solutions were added to the distilled water and the gel was kept in there to stain for 30 minutes to prevent hampering in intercalation and later visualized using a transilluminator.

Molecular Docking Study

For this study, the structure of compounds was drawn in Chem Bio Ultra 6.0 tool and converted into .pdb format by using Chem Bio 3D Ultra 6.0. 3D structure of chloramphenicol was obtained from PubChem. The crystal structure of bacterial proteins was downloaded from *RCSB* protein data bank with PDB IDs [*Escherichia coli* (PDB ID: 3T88), *Staphylococcus aureus* (PDB ID: 3TY7), *Bacillus subtilis* (PDB ID: 5H67) and *Pseudomonas aeruginosa* (PDB ID: 3P3E).[29] While, 3D structure of DNA was obtained with PDB ID: 1BNA for DNA binding study. The downloaded 3D structures were further processed and prepared for molecular docking by using Discovery Studio Visualizer. PyMOL software package and Discovery Studio Visualizer were used for the visualization of the docking results.[30,31] Molecular docking studies were carried out with the AUTODOCK 4.2 tool. The excess solvents and water molecules were removed from the proteins and the polar hydrogen bonds, Kollman untied atoms type charges were added.[32] Incidentally, the root of the ligand was positioned and its orientation and torsion were also set. *In silico* ADMET limits were studied with pre-ADMET online tool.

RESULTS AND DISCUSSION

Structural Confirmation and Analytical Data Physiochemical Property

Table-1 consists of the result of elemental analysis which was in good agreement with the predicted molecular formula of ligand and its metal (II) ions in the ratio of 2:1.

Mass Spectra of *N*-(8-hydroxyquinolin-5-yl)-4-methylbenzenesulfonamide (8HQMBS)

Fig-1 and 2 represent the mass spectrum of 8HQMBS ligand and its $Fe(8HQMBS)_2(H_2O)_2$ complex. In the mass spectrum of 8HQMBS, the molecular ion peak at 313.17 m/z with the greatest intensity i.e. of 92% relative abundance corresponds to our target molecule 8HQMBS with a molecular weight 314.35.

While, in the spectra of $Fe(8HQMBS)_2(H_2O)_2$ complex, the peak at 720.93 m/z is the molecular ion peak of the complex, the peak at 315.48 m/z is of 8HQMBS ligand present in the complex and the peak at 161.45 m/z with 100% relative abundance is the fragment of 5-amino-8-hydroxyquinoline. From all these data we can say that the target molecules have been synthesized.

Table-1: Physiochemical Property of 8HQMBS Ligand and its Metal Complexes

Compound Name (Chemical Formula)	Mol. weight	Yield (%)	M.P. (°C)	Colour	Elemental Analysis, % found (required)				
					C	H	N	S	Metal
8HQMBS ($C_{16}H_{14}N_2O_3S$)	314.36	78	220	Buff	61.05 (61.13)	4.52 (4.49)	8.85 (8.91)	10.0 (10.20)	---
$Mn(8HQMBS)_2(H_2O)_2]$ ($C_{32}H_{30}MnN_4O_8S_2$)	719.66	68.66	257-259	Brown	53.28 (53.56)	4.40 (4.21)	7.76 (7.81)	8.35 (8.93)	7.79 (7.66)
$Fe(8HQMBS)_2(H_2O)_2]$ ($C_{32}H_{30}FeN_4O_8S_2$)	720.57	66.66	264-266	Black	53.33 (53.49)	4.12 (4.21)	7.50 (7.80)	8.35 (8.92)	7.22 (7.77)
$Co(8HQMBS)_2(H_2O)_2]$ ($C_{32}H_{30}CoN_4O_8S_2$)	723.65	63.33	268-270	Dark yellow	53.16 (53.26)	4.65 (4.19)	7.36 (7.76)	8.28 (8.89)	8.55 (8.17)
$Ni(8HQMBS)_2(H_2O)_2]$ ($C_{32}H_{30}NiN_4O_8S_2$)	723.41	73.33	268-269	Greenish Yellow	53.12 (53.28)	4.45 (4.19)	7.57 (7.77)	8.52 (8.89)	8.54 (8.14)
$Cu(8HQMBS)_2(H_2O)_2]$ ($C_{32}H_{30}CuN_4O_8S_2$)	728.27	88.67	272-273	Yellowish Green	52.59 (52.92)	4.69 (4.16)	7.35 (7.71)	8.31 (8.83)	8.25 (8.75)
$Zn(8HQMBS)_2(H_2O)_2]$ ($C_{32}H_{30}ZnN_4O_8S_2$)	728.1	70	282-284	Light yellow	52.52 (52.79)	4.82 (4.15)	8.15 (7.69)	8.69 (8.81)	8.92 (8.96)

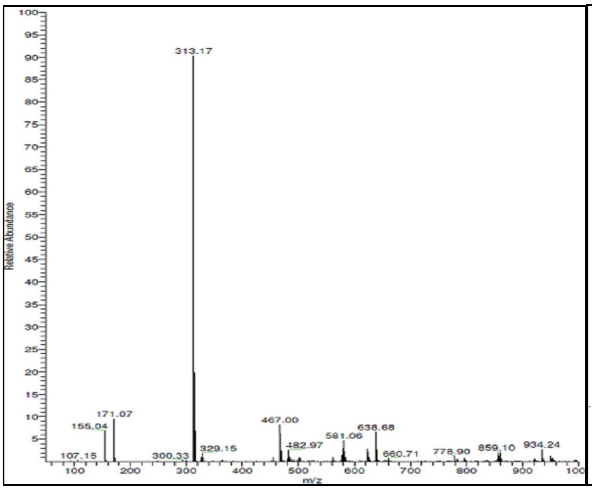

Fig-1: Mass Spectra of 8HQMBS Ligand

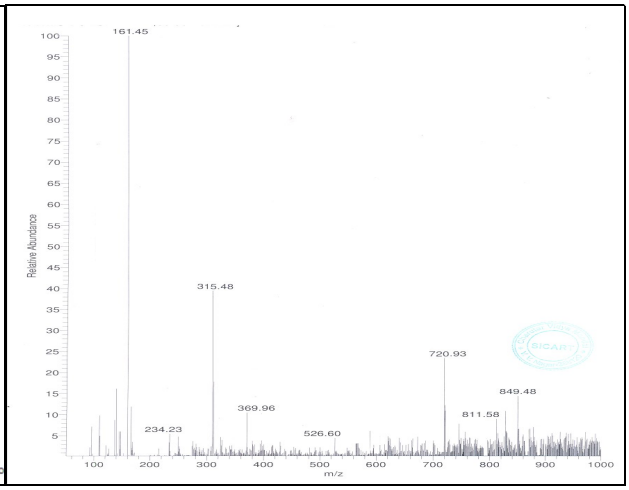

Fig-2: Mass Spectra of $Fe(8HQMBS)_2(H_2O)_2$ Complex

FT-IR Data Analysis of 8HQMBS Ligand and its Metal Complexes

The IR spectra of synthesized ligand and its metal complexes were recorded and their tentative assignments are discussed here. A band observed at 3431 cm^{-1} in the spectrum of 8HQMBS was due to O–H stretching vibrations and a sharp band at 1493 cm^{-1} were due to O–H bending vibration.[33] A sharp band at 1152 cm^{-1} was attributed to C–O stretching in free ligand and the $–CH_2–$ showed C–H stretching vibration at 2925 cm^{-1}.[33] Also, the IR spectrum of 8HQMBS showed some important bands at 1620 cm^{-1} of C=C, at 1572 cm^{-1} of C=N and 1457 cm^{-1} of C–C, indicate the aromatic skeletal stretching vibrations of the parent heterocyclic ring.[33] Further, a sharp band observed at 1352 cm^{-1} was assigned to S=O of –

SO_2NH_2 which confirmed the synthesis of 8HQMBS ligand.[34] However, on coordination with metal salts, the FT-IR spectra of 8HQMBS metal complexes showed some important characteristic differences. The significant difference to be expected was the presence of a broad band in the region of 3410 cm^{-1} to 3425 cm^{-1} of metal complexes, as the oxygen of the –OH group of the ligand formed a coordination bond with the metal ions. This clears the participation of the free –OH group in bond formation with the central metals. The other noticeable difference was the shifting of the band at 1620 cm^{-1} due to C=N stretching vibration of 8-hydroxyquinoline moiety in 8HQMBS ligand to the lower frequencies, whereas the band at 1457 cm^{-1} assigned to in-plane –OH deformation was also shifted to lower frequencies in the spectra of metal complexes due to the formation of M–O bond.[23] Similar peaks were observed between the ranges of 1340 cm^{-1} to 1345 cm^{-1} in the spectra of metal complexes which was due to the presence of $–SO_2NH_2$ group in the structures.[35] The weak band around ~1110 cm^{-1} was due to C–O–M stretching while the bands around ~750 cm^{-1} and ~530 cm^{-1} were assigned to M→N bond formation in the complex structure.[36] These characteristic features of the IR studies suggest the formation of 8HQMBS and its metal complexes. Also, the colour changes after complex formation are in agreement that the complexation of metal and ligand took place successfully. The FT-IR spectra of ligand 8HQMBS and its metal complexes are represented in Fig.-3.

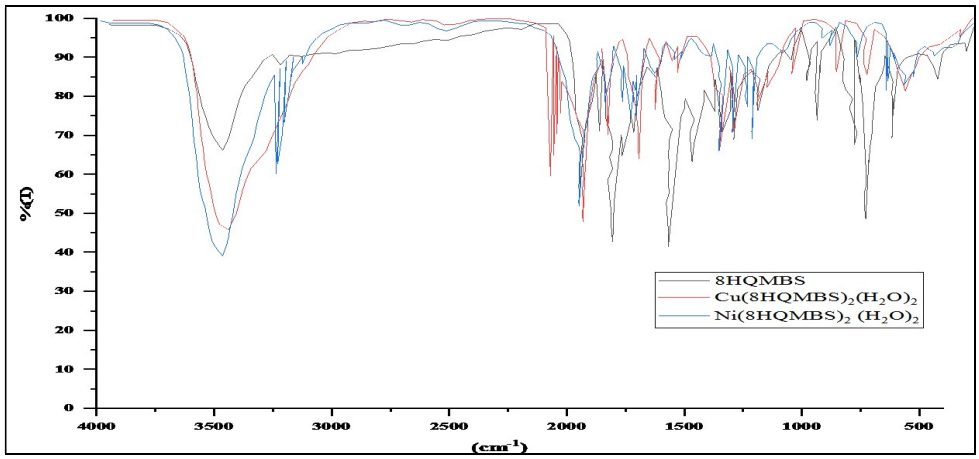

Fig.-3: FT-IR Spectrum of 8HQMBS Ligand and its Ni(II) and Cu(II) Metal Complexes

^{1}H-NMR Spectra

The structure of 8HQMBS ligand and its $Zn(8HQMBS)_2(H_2O)_2$ complex were characterized by ^{1}H-NMR analysis in DMSO-d_6 system. The obtained spectra are shown in Fig.-4 and Fig.-5 respectively**.** The ^{1}H-NMR (400 MHz, DMSO-d_6, δ_H, ppm) of 8HQMBS ligand was assigned as follows: 11.05 (1H of $–SO_2N\underline{H}–$ of the sulphonamide group), 9.208 (1H, of Aromatic –OH), 8.98, 7.80, 8.12 (3H of the pyridine ring), 7.97-7.95 (2H of the aromatic ring next to sulphonamide linkage) 7.73- 6.83 (2H of the phenolic ring), 7.49- 7.47 (2H of the aromatic ring near the carbon atom with methyl group), 2.29 (belongs to 2H of methyl group attached to an aromatic ring). A typical downfield shift was observed in the spectra of the $Zn(8HQMBS)_2(H_2O)_2$ complex. The peak belonged to aromatic –OH in the spectra of ligand was disappeared in the spectra of $Zn(8HQMBS)_2(H_2O)_2$ complex evident the participation of –OH group in bond formation with the metal ion at the center.[37]

^{13}C-NMR spectra of 8HQMBS

The ^{13}C-NMR spectra of 8HQMBS ligand consist of peaks between δ 115.64-148.06 ppm which belongs to all the aromatic carbons and the peak of CH_3 group in the structure appeared at δ 20.75 ppm. ^{13}C-NMR spectrum of 8HQMBS ligand is represented in Fig.-6.

Electronic Spectra and Magnetic Moment Data

The electronic spectra of 8HQMBS ligand and its metal complexes were measured between 200 to 800 nm in DMSO in 3 mmol solutions and the obtained data are listed in Table-2 and Fig.-7. The absorption bands for ligand and metal complexes were observed with different intensities.

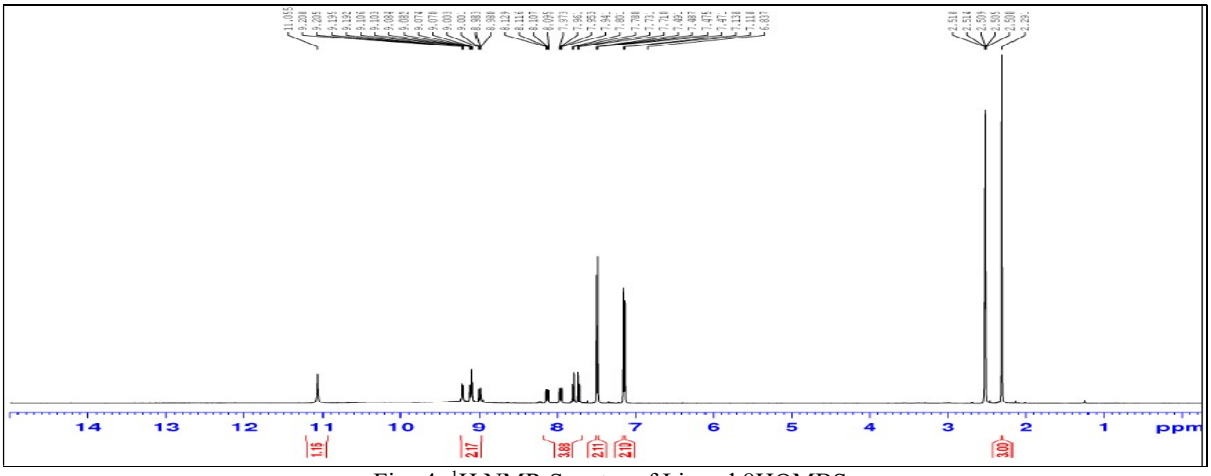

Fig.-4: ^{1}H NMR Spectra of Ligand 8HQMBS

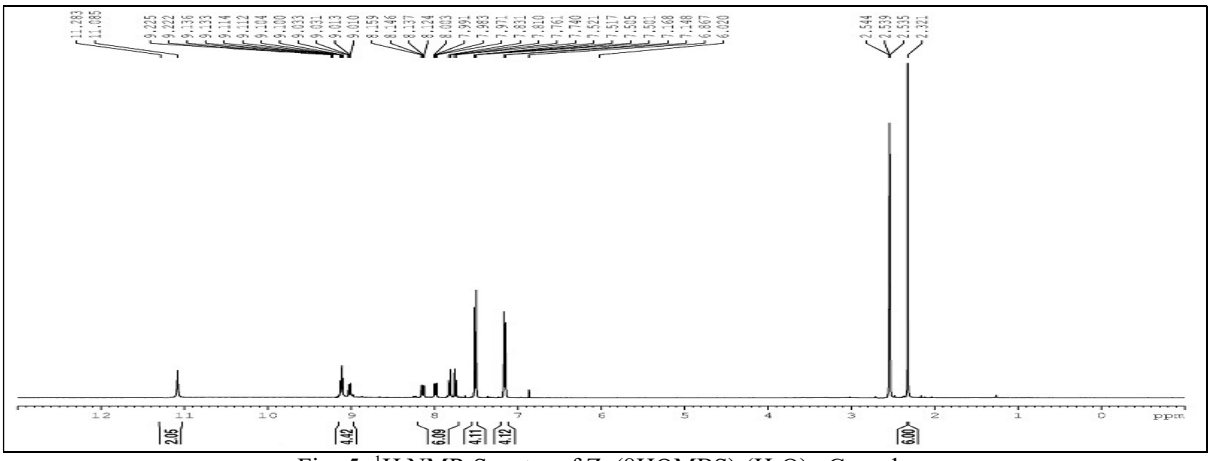

Fig.-5: ^{1}H NMR Spectra of $Zn(8HQMBS)_2(H_2O)_2$ Complex

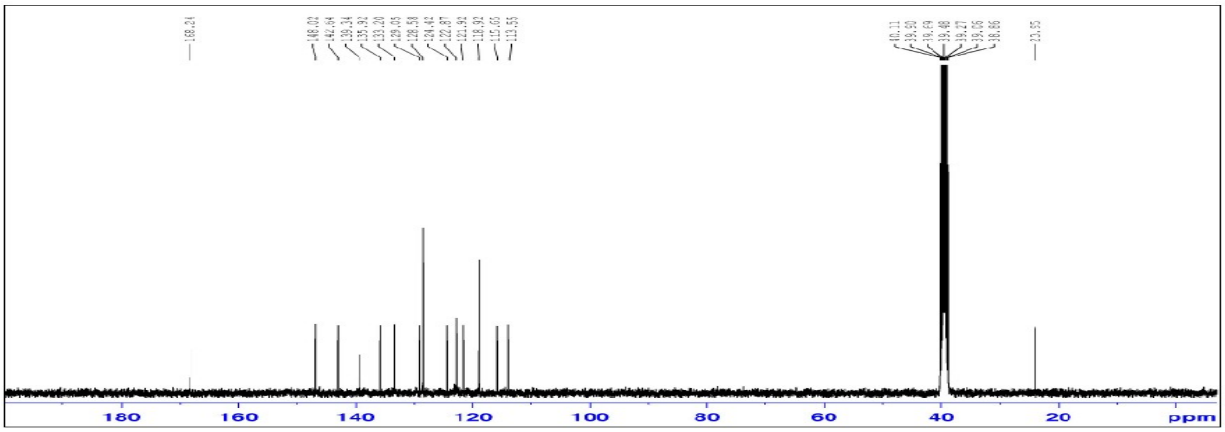

Fig.-6: ^{13}C NMR Spectra of 8HQMBS Ligand

The free ligand exhibit a strong absorption band at 320 nm, which is attributed to the conjugated ring π→ π* transition. Less intense bands at 390 nm and 485 nm are due to n→ π* transition of conjugated quinoline rings.[38] A noticeable band shift was observed in the UV spectra of metal complexes. The emerging absorbance in the visible range (320-360 nm) of the metal complexes is attributed to π→ π* transition. The less intense band at 428, 426, 475, and 370 nm of Cu(II), Zn(II), Co(II), and Fe(II) metal complexes respectively is due to typical charge transfer transition between ligand field.[38] The Cu(II)

complex exhibits broadband at 640 nm due to $^2E_2g \rightarrow {}^2T_2g$ normal transition and the magnetic moment 1.56 B.M. corresponding to one unpaired electron indicating its distorted octahedral geometry.[38] A broad peak to the higher side (bathochromic shift) at 640 and 633 nm of Mn(II) and Ni(II) as shown in Fig.-7 was due to the $^4T_{1g}(F) \rightarrow {}^4T_{1g}\,{}^5T_2$ and $^4T_{1g}(F) \rightarrow {}^4T_{1g}$ transitions respectively. This shows the formation of octahedral geometry. Also, the results of magnetic moment listed in Table-2 were shown to have octahedral geometry for all the M(II) complexes.[39] The complexation obtained by deprotonation of phenolic group of 8-hydroxyquinoline is characterized by such kind of peaks. The magnetic susceptibility test was conducted at room temperature. The magnetic values obtained for Ni(II) and Co(II) complexes at 3.05 and 3.75 BM is typical for octahedral geometry.[40] The values obtained at 5.84 and 4.52 for Mn(II) and Fe(II) were due to the octahedral geometry of the complexes. [40] The Zn(II)complex is diamagnetic.

Thermogravimetric Analysis Data of 8HQMBS Ligand and its Metal Complexes

Thermogravimetric analysis (TGA) was carried out to check the thermal stability of the synthesized ligand and its metal complexes and to find the nature of water molecules associated with it. The analysis was carried out in the temperature range 50-600 ºC in the air at a heating rate of 10 ºC per minute. The thermogram curve of all the compounds is represented in Fig.-8. The change in percentage mass losses accompanying the changes in heating revealed the following findings. The first decomposition was observed in the range of 110 ºC to 150 ºC with 5-6% weight loss that explains the loss of water molecules in coordination.[36] In the thermogram curves of metal complexes the most weight loss of around 75-80% was observed in the temperature range 200-400 ºC corresponds to the decomposition of bidentate ligand leaving behind the metal oxinates.[36] The remaining 20% weight loss is observed in a slow decomposition pattern in the range of 400-600 ºC which may correspond to a mixture of metal oxide and some ashes as the final residue.[41] A noticeable difference in the degradation mode of 8HQMBS and its metal complexes had been observed. 8HQMBS ligand showed a steady, one-step degradation pattern as compared to metal complexes of 8HQMBS.

Table-2: UV-Vis Absorption Data of 8HQMBS Ligand and its Metal Complexes (3 mmol solutions in DMSO)

Compound Name	λnm	Transition	Suggested structure	μeff B.M.
8HQMBS	320 390 485	π→ π* n→ π* n→ π*	--	---
$[Mn(8HQMBS)_2(H_2O)_2]$	362 428 640	π→ π* L→M $^4T_{1g}(F) \rightarrow {}^4T_{1g}$	Octahedral	5.84
$[Fe(8HQMBS)_2(H_2O)_2]$	322 370 465 620	π→ π* Ligand field $^5T_2g \rightarrow {}^5Eg(D)$ $^5T_2g \rightarrow {}^5Eg(D)$	Octahedral	4.52
$[Co(8HQMBS)_2(H_2O)_2]$	323 379 475 690	π→ π* L→M L→M $^4T_{1g}(F) \rightarrow {}^4T_{2g}(F)$	Octahedral	3.75
$[Ni(8HQMBS)_2(H_2O)_2]$	362 395 633	π→ π* $^3A_{2g}(F) \rightarrow {}^3T_{1g}(P)$ $^3A_{2g}(F) \rightarrow {}^3T_{2g}(F)$	Octahedral	3.05
$[Cu(8HQMBS)_2(H_2O)_2]$	362 428 640	π→ π* L→M $^2B_1g \rightarrow {}^2Eg$	Distorted Octahedral	1.56
$[Zn(8HQMBS)_2(H_2O)_2]$	362 426 640	π→ π* L→M L→M	Octahedral	D

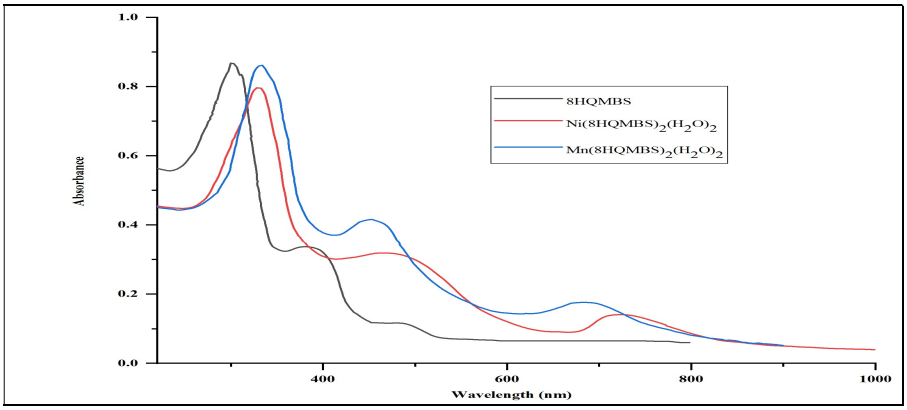

Fig.-7: UV Absorption Spectra of Ligand 8HQMBS and its Ni(II), Mn(II) Complex

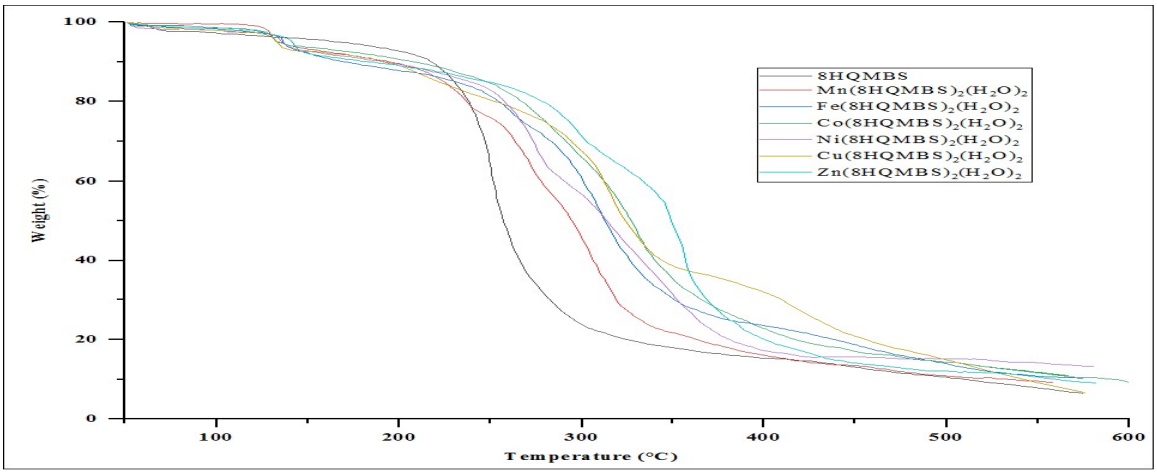

Fig.-8: TGA Spectrum of Ligand 8HQMBS and its Metal Complexes

In vitro Antimicrobial Activity

The synthesized 8HQMBS ligand and its metal complexes were investigated for their *in vitro* activity against pathogenic bacterial and fungal strains. For this study, two Gram+ve (*Staphylococus aureus* and *Bacillus subtilis*) and two Gram-ve (*Pseudomonas aeruginosa* and *Escherichia coli*) bacterial strains were used. For antifungal activity, *Aspergillus niger* and *Aspergillus flavus* fungal strains were used. Antimicrobial activity was investigated by "Broth Dilution Method" method. The MIC (minimal inhibitory concentration) value was read to check the correct concentration of the drug that is required to control organism growth. The lowest concentration at which the growth was inhibited was recorded as the MIC. The MIC values of the newly synthesized compounds were compared with standard drugs (ampicillin, chloramphenicol, nystatin, and griseofulvin) and the results are summarized in Table-3.

The results suggested that the antimicrobial potency of 8HQMBS ligand increases upon metal complexation. The probable reason could be due to the substitution of sulfonamide group on the 5th position of 8-hydroxyquinoline and the increased lipophilicity behaviour of metal complexes. The bactericidal activity was higher in Gram+ve bacteria as compared to the Gram-ve bacteria because 8HQMBS ligand has 8-hydroxyquinoline as parent moiety which complexes the metal ion to form a lipophilic complex which aids in the transportation of the compound inside the cell membrane of Gram+ve bacteria. Whereas the effect on Gram-ve bacteria was less, maybe due to the selective transport barrier of its cell wall. Antifungal activity was moderate.

The biological activity of the ligands and their metal complexes depends on ligands property, lipophilicity, nature of metal ion, its coordination state, and geometry of the complex. The activity of coordinate compounds may be due to their lipophilic behaviour which allows it to penetrate inside the cell

wall and exert its activity through oxidation stress or binding with the enzyme's metal-binding site and blocking its activity.[42]

Table-3: *In vitro* Antimicrobial Activity (MIC, µg/mL) of Ligand and its Metal Complexes

Compounds	Gram-positive Bacteria		Gram-negative Bacteria		Fungi	
	S. aureus (MTCC-96) *µg/mL*	*B. subtilis* (MTCC 441) *µg/mL*	*E. Coli* (MTCC 443) *µg/mL*	*P. aeruginosa* (MTCC-1688) *µg/mL*	*A. niger* (MTCC 282) *µg/mL*	*A. flavus* (NRRL-21882) *µg/mL*
8HQBMS	900	1500	1000	800	1000	800
$[Mn(8HQMBS)_2(H_2O)_2]$	200	200	300	450	300	500
$[Fe(8HQBMS)_2(H_2O)_2]$	100	150	50	200	200	150
$[Co(8HQBMS)_2(H_2O)_2]$	250	350	300	400	250	250
$[Ni(8HQBMS)_2(H_2O)_2]$	100	100	150	200	200	100
$[Cu(8HQBMS)_2(H_2O)_2]$	50	100	50	150	150	100
$[Zn(8HQBMS)_2(H_2O)_2]$	300	500	800	550	500	300
Ampicillin	250	200	100	100	---	---
Chloramphenicol	50	100	50	50	---	---
Nystatin	---	---	---	---	100	100
Griseofulvin	---	---	---	---	100	400

DNA Binding Studies

Viscosity Measurement

Hydrodynamic measurements that are sensitive to length change (i.e., viscosity and sedimentation) are considered as one of the least uncertain and most critical tests in the absence of crystallographic structural data to study the binding model in a solution. So, to confirm the DNA binding mode, a viscosity study was carried out. When there is classical intercalation, the viscosity of the solution increases, because during the process lengthening of the DNA helix occurs, as the base pairs separate to accommodate the binding complex. Whereas in partial, non-classical intercalation the viscosity decreases due to bending or nicking of DNA helix which further reduces the length of the DNA helix. And no alteration in the viscosity of DNA solution is observed in the case of groove or electrostatic binding. A covalent binding leads to the scission of DNA helix causes a decrease in its length which in turn decreases the viscosity of the solution. A significant increase in the relative viscosity was observed upon the addition of metal complexes in the DNA solution proves the intercalation binding nature of the compounds. The results are compared with the classical DNA intercalator (ethidium bromide). The graph plot of $(\eta/\eta_0)^{1/3}$ *vs*. [DNA] / [complex] in Fig.-9 gives a measure of the viscosity change.[43]

UV-Vis Experiment

The absorption titration study was carried out to elucidate the binding mode of compounds with DNA strands. Through UV absorption spectroscopy, the interaction of ligand and its transition metal complexes was investigated in the absence and presence of an increasing concentration of DNA and a fixed concentration of complexes (10 µl). A noticeable hypochromism or redshift is usually characterized as non-covalent intercalation binding of the compound to the DNA helix. This is due to the strong $\pi \rightarrow \pi$ stacking interaction between the aromatic chromophore of the compound and DNA base pairs. In Table-4,

the results of absorption titration of DNA with metal salts and with the ligand or its metal complexes are given. There was a remarkable difference in the wavelength of the complexes titrated with DNA in comparison to their specific metal salts and ligand. The wavelength is shifted towards the right (redshift) which states the intercalation binding mode.[44]

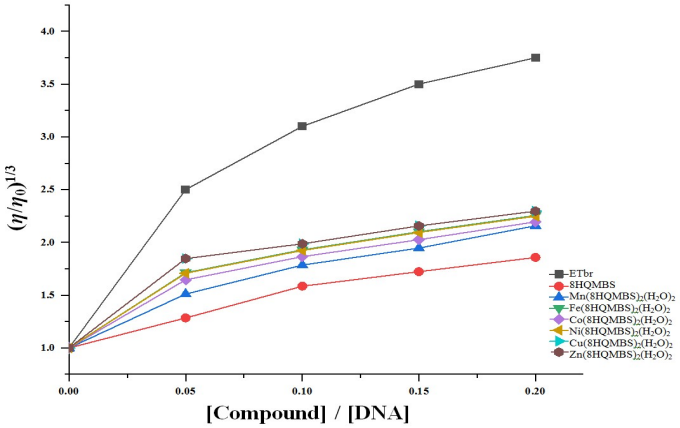

Fig.-9: Measurements of the Viscosity of Metal Complexes on binding with CT-DNA

Table-4: Absorption Titration Data with Ligand and its Metal Complexes with DNA

Compound (10 µl)	DNA (µl)	Complexes λmax (nm)	8HQMBS ligand λmax (nm)	M(II) λmax (nm)
$[Mn(8HQMBS)_2(H_2O)_2]$	0	273.9	262.2	265.5
	4	265.9	261.2	262.9
	8	263.1	260.5	262.2
	12	261.4	260.2	261.5
$[Fe(8HQMBS)_2(H_2O)_2]$	0	275.5	262.2	266.2
	4	269.3	261.2	264.5
	8	265.5	260.5	262.7
	12	264.1	260.2	261.2
$[Co(8HQMBS)_2(H_2O)_2]$	0	274.6	262.2	265.5
	4	268.7	261.2	262.4
	8	264.3	260.5	261.4
	12	262.5	260.2	260.5
$[Ni(8HQMBS)_2(H_2O)_2]$	0	278.5	262.2	265.8
	4	266.5	261.2	263.5
	8	264.2	260.5	262.7
	12	263.4	260.2	261.5
$[Cu(8HQMBS)_2(H_2O)_2]$	0	279.8	262.2	270.3
	4	271.2	261.2	268.2
	8	268.7	260.5	266.1
	12	265.2	260.2	262.4
$[Zn(8HQMBS)_2(H_2O)_2]$	0	278.7	262.2	268.5
	4	270.1	261.2	266.3
	8	267.3	260.5	265.2
	12	264.5	260.2	263.3

DNA Binding Study through Gel Electrophoresis (Gel Retardation Assay)

Gel electrophoresis is a useful tool to investigate the mobility of DNA in the agarose gel environment on the influx of electric potential. In the present study, change in the electrophoretic migration of DNA in the

absence and presence of complexes is taken as the proof of complex DNA-interaction. The more delay in the time of migration than DNA is usually considered as the confirmation of complex-DNA interaction. Delay in migration time of DNA was due to the rise in the molecular weight, size, and shape after interaction with complexes. The electro-phoretogram represented in Fig.-10 shows that the complex interaction slows down the migration of DNA which visibly proves the complex-DNA interaction via intercalation.[45]

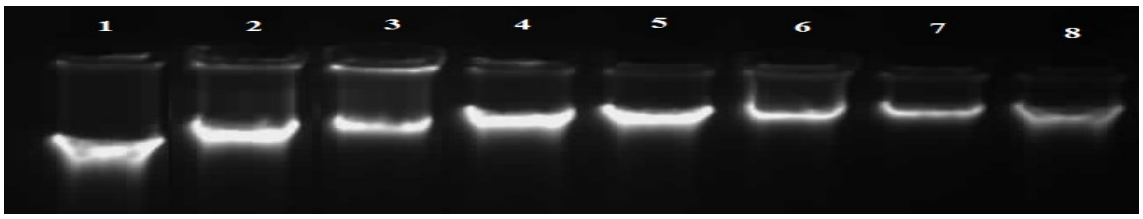

Fig.-10: Agarose Gel Electrophoresis Image Consisting of CT-DNA = Lane-1, 8HQMBS = Lane-2 and Lane 3-8 are of Mn(II), Fe(II), Co(II), Ni(II), Cu(II), and Zn(II) Metal Complex respectively

Computational Studies

***In silico* Antibacterial Studies**

Molecular docking is one of the rational drug design and biological systematic technique which is used to define the type of interaction, inhibitor potential or the mechanism of the chemical entity in the receptor. The molecular docking was performed using AUTODOCK version 4.2 and the results were visualized using PyMol and Discovery Studio Visualizer. *In silico* antibacterial studies were carried out on microorganism's proteins such as *Escherichia coli* (PDB ID: 3T88), *Staphylococcus aureus* (PDB ID: 3TY7), *Bacillus subtilis* (PDB ID: 5H67) and *Pseudomonas aeruginosa* (PDB ID: 3P3E) to provide detailed insight on binding sites and the type of interactions.[29] This study will also serve as supporting data for *in vitro* antibacterial studies. The molecular docking results of the synthesized 8HQMBS ligand and its metal complexes with bacterial proteins are represented in terms of binding affinity (kcal/mol). The obtained results of synthesized compounds are compared to that of standard drug chloramphenicol and are summarized in Table-5. 8HQMBS ligand and its metal complexes showed good binding affinity than chloramphenicol with the protein receptor which suggests their better fit in the receptors cavity. 3D and 2D images of 8HQMBS and its metal complex docked with protein are shown in Fig.-11. The results are in concordance with *in vitro* studies wherein the metal complexes are binding strongly to 8HQMBS ligand and chloramphenicol.

Molecular Docking

For molecular interaction study of synthesized compounds with DNA helix, blind docking was performed on DNA helix with sequence (CGCGAATTCGCG), PDB ID: 1BNA. The grid map along the x, y, and z axes was set to 30×26×30 $Å^3$ with 1.0Å grid spacing. Before docking, all the synthesized compounds serving as ligand were saved in .pdb format by using Chem-Bio 3D Ultra 6.0. 3D. Each of the ligands was further characterized by its seven 2D descriptors (molecular weight, AlogP, number of hydrogen bond acceptors or donors, number of rotatable bonds, number of rings and aromatic rings) and the Gesteiger charges were added which is the default partial charges of AUTODOCK program.[46] Two DNA strands colliding together form two different grooves in the B-DNA which run parallel to the backbone named as the minor and major groove. The ligands bind to both the grooves by hydrogen bonds but the major groove binders utilize exposed methyl grooves in the T region.[9] This difference leads to the selectivity of the groove in which protein and large nucleotides bind to the major groove and small molecules bind preferably to the minor groove. Several minor groove binders have been shown to prefer AT-rich sequences because these regions are narrower and slightly deeper than GC-rich regions, enabling better ligand fit.[9]

Intercalation is the most common binding mode of small aromatic molecules. Intercalation is the introduction of small molecules or fragments between two adjacent DNA strand base pairs, either with or without extra groove interactions (threading intercalation or classical intercalation).[9] The binding mode of

intercalation includes a gap opening between the stacked base pairs that result in the formation of a hydrophobic pocket.

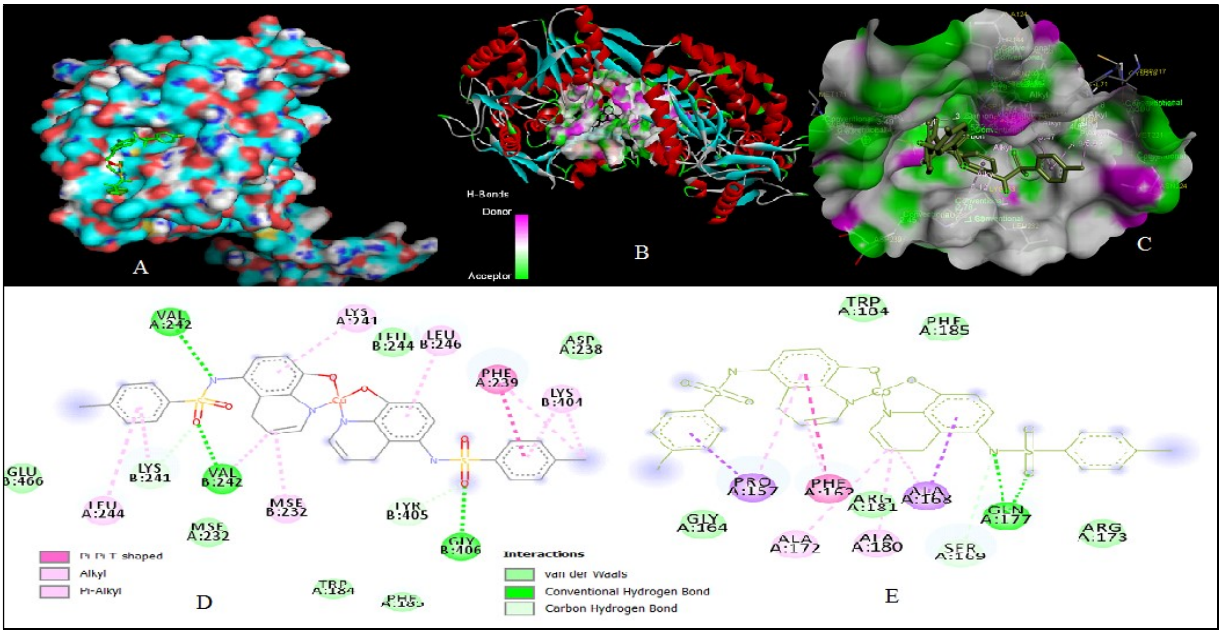

Fig.-11: A and B;= 3D Interaction View with Bacterial Protein, C;= 3D Interaction by Hydrogen Bonding, D & E;= 2D view of Cu(II) and Co(II) Metal Complexes docked with Bacterial Protein (PDB:ID 3t88)

Table-5: *In silico* Molecular Docking Studies of 8HQMBS Ligand and its Metal Complexes with Bacterial Proteins in terms of Binding Affinity concerning Standard Drug Chloramphenicol

Compound	Binding Affinity for Different Proteins (kcal/mol)			
	5H67	3TY7	3T88	3P3E
8HQMBS	-7.6	-7.5	-7.1	-7.4
$[Mn(8HQMBS)_2(H_2O)_2]$	-9.9	-10.0	-10.1	-9.6
$[Fe(8HQMBS)_2(H_2O)_2]$	-9.1	-10.1	-9.2	-9.5
$[Co(8HQMBS)_2(H_2O)_2]$	-8.3	-9.9	-7.0	-9.2
$[Ni(8HQMBS)_2(H_2O)_2]$	-9.2	-9.4	-9.1	-10.0
$[Cu(8HQMBS)_2(H_2O)_2]$	-9.7	-10.0	-9.2	-10.0
$[Zn(8HQMBS)_2(H_2O)_2]$	-10.2	-10.0	-10.0	-10.1
Chloramphenicol	-7.2	-6.9	-6.9	-7.5

The insertion of most intercalating ligands occurs into the CG intercalation site. Ligands containing a polyaromatic planer system forms π→π interaction with the two flanking bases and intercalate, which is the main driving force of intercalation binding mode. Another intercalation occurs through Van der Walls, hydrogen bonding, and charge-transfer interactions.[9] It was observed that many intercalates are positively charged due to the important contribution of electrostatics to the binding energy. The result of the docking model showed that the synthesized compounds interact with DNA into the GC-rich region by the formation of hydrogen bonds and π→π interactions. This confirms the intercalation binding mode as shown in Fig.-12. The binding energy of all the complexes was > -10 kcal/mol which tells us that their binding ability is good with DNA helix.

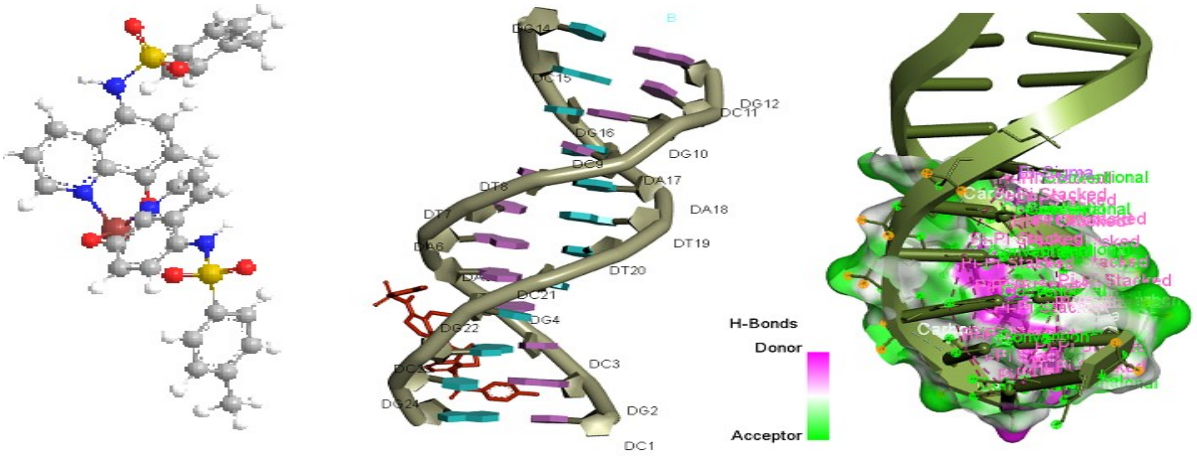

Fig.-12: Threading Intercalation of Ligand Cu Complex (Stick Presentation) is shown in Orange Color with DNA (PDB ID: 1BNA)

ADMET Properties Prediction by Online *Pre*-ADMET Tool

The *in silico* ADMET (absorption, distribution, metabolism, excretion and toxicity) properties of the synthesized compounds were screened on *Pre*-ADMET, a web-based application. The predicted ADME values illustrate the physiochemical properties and the drug-like nature of the newly synthesized compound. For a compound to be considered as a drug candidate, it should follow Lipinskis rule of five (Molecular weight ≤ 500 (g/mol), Hydrogen Bond Acceptor ≤ 10, logP ≤ 5, Hydrogen Bond Donor ≤ 5) and have strong absorption. The screening of absorption property is important in ADMET profiling as it indicates the bioavailability of the drug which correlates the drug efficiency. 8HQMBS ligand meets all the need of Lipinski rule, whereas only one rule is violated in case of metal complexes as their molecular weight are >500. Tropical polar surface area (TPSA) values help in the correlation with passive transportation of drugs through the phospholipids bilayer membrane. TPSA value of ligand and metal complexes are below 140 Å which falls under the permeability index. The predicted values and related ADMET properties are shown in Table-6 and Table-7.

Table-6: Evaluation of Pharmacokinetic Parameters of Molecules

Compound	Molecular Weight	LogP	LogS	H-Acceptors	H-Donors	TPSA
8HQMBS	314.36	1.880	-3.81	4	2	87.670
$[Mn(8HQMBS)_2(H_2O)_2]$	719.66	3.568	-8.29	6	2	135.32
$[Fe(8HQMBS)_2(H_2O)_2]$	720.57	0.845	-8.33	6	2	135.32
$[Co(8HQMBS)_2(H_2O)_2]$	723.65	0.845	-8.32	6	2	135.32
$[Ni(8HQMBS)_2(H_2O)_2]$	723.41	0.845	-8.31	6	2	135.32
$[Cu(8HQMBS)_2(H_2O)_2]$	728.27	0.845	-8.34	6	2	135.32
$[Zn(8HQMBS)_2(H_2O)_2]$	728.10	0.845	-8.36	6	2	135.32

[(The BBB (Blood Brain Barrier): Low absorption to CNS <0.1, High absorption CNS >2.0, Middle absorption CNS 2.0-0.1; Caco2 (human colon carcinoma cell line): High permeability >70, Middle permeability 4-70, Low permeability <4; %PPB (Plasma Protein Binding): Strongly Bound >90%, Weakly Bound <90%, %HIA (Human Intestinal Absorbance): Well absorbed compounds 70-100%, Moderately absorbed compounds 20-70%, Poorly absorbed compounds 0-20%; MDCK (Madin-Darby

Canine Kidney cell line): Higher permeability >500, Medium Permeability 25-500, lower permeability <25).[47-49] The association between BBB, %HIA, Caco2, %PPB and MDCK has been studied. The result suggests that all the synthesized compounds have low absorbance to CNS, middle permeability to Caco2 and good human intestinal absorbance. 8HQMBS and $Cu(8HQMBS)_2(H_2O)_2$complex showed strong binding to plasma protein and rest are moderately bound and have low penetrance to MDCK cells which overall states that the synthesized ligand and complexes have good ADME properties. None of the synthesized compounds showed any sign of toxicity *in silico.* So, they can be considered as good drug candidates.

Table-7: Evaluation of ADMET Parameters of Molecules

Compound	%HIA	%PPB	BBB	Caco2 (nm/sec)	MDCK (nm/sec)	Toxicity(Tumorogent/ Carcinogent/ Irritant)
8HQMBS	94.300	98.387	0.264	2.010	8.796	None
$[Mn(8HQMBS)_2(H_2O)_2]$	98.537	66.794	0.041	21.979	0.367	None
$[Fe(8HQMBS)_2(H_2O)_2]$	97.954	81.924	0.151	12.268	0.045	None
$[Co(8HQMBS)_2(H_2O)_2]$	97.955	81.839	0.151	13.140	0.044	None
$[Ni(8HQMBS)_2(H_2O)_2]$	97.979	88.112	0.151	12.422	0.044	None
$[Cu(8HQMBS)_2(H_2O)_2]$	97.955	97.955	0.151	13.376	0.036	None
$[Zn(8HQMBS)_2(H_2O)_2]$	97.955	81.721	0.151	14.106	0.030	None

CONCLUSION

In the present study, a new *N*-(8-hydroxyquinolin-5-yl)-4-methylbenzenesulfonamide (8HQMBS) ligand and its metal complexes were synthesized and well characterized. Thermal analysis, magnetic susceptibility and UV-Visible study suggested the octahedral geometry of metal complexes. *In vitro* antibacterial and antifungal screening results showed that 8HQMBS ligand and its metal complexes have good antimicrobial potential. The Cu(II), Fe(II) and Ni(II) metal complexes showed better antibacterial and antifungal potential than Zn(II), Mn(II) and Co(II) complexes. Also, DNA binding mode was studied by various spectral analyses and gel electrophoresis which showed intercalation type of binding. Finally, the *in silico* studies also supported the experimental results. *In silico* binding properties of the compounds on bacterial proteins in comparison to the standard drug, chloramphenicol was studied in terms of binding affinity. The binding affinities of all the compounds were better than chloramphenicol. Moreover, *silico* docking studies with B-DNA (1BNA) also showed intercalation binding mode. *In silico* ADMET study showed good ADMET properties of the compounds as all the parameters were found within the permissible range concluding that the tested molecules can be considered as good drug candidates.

ACKNOWLEDGEMENT

The authors are thankful to Charutar Vidya Mandal, Vallabh Vidyanagar and Head, ARIBAS for providing research facility. One of the authors, Ruby Kharwar also gratefully acknowledges the Ministry of Tribal Affairs Government of India for providing financial support under the National Fellowship Scheme For Higher Education of ST Students [Ref. No.: NFST-2015-17-ST-GUJ-1735]. The service of SICART, Vallabh Vidyanagar, for NMR and MASS, FTIR analysis and PDPIAS, CHARUSAT for TGA analysis is gratefully acknowledged.

REFERENCES

1. O'Driscoll and M. Clynes, *Chemotherapy,* **52(3)**, 125(2006), **DOI:**10.1159/000092540
2. Y. Minagawa, J. Kigawa, H. Itamochi, Y. Kanamori, M. Shimada, M. Takahashi and N. Terakawa *Japanese Journal of Cancer Research*, **90(12)**, 1373(1999), **DOI:**10.1111/j.1349-7006.1999.tb00722.x

3. N. Umar, N. Mhlongo, and M. E. Soliman, *Drug Design, Development and Therapy,* **11**, 599 (2017), **DOI:**10.2147/DDDT.S119488
4. P. Rahul, and P. J. Hergenrother, *Current Opinion in Biotechnology*, **18(6)**, 497(2007), **DOI:**10.1016/j.copbio.2007.09.006
5. H. Wu, F. Shi, Wang, X. Zhang, Y. Bai, Y. Kong, J. Wang, *Transition Metal* Chemistry, **39(3)**, 261(2014), **DOI:**10.1007/s11243-014-9799-8
6. T. Takagaki, T. Bando, *Journal of American Chemical Society,* **134(31)**, 13074(2012), **DOI:**10.1021/ja3044294
7. M. P. Barrett, C. G. Gemmell and C. J. Suckling, *Pharmacology & Therapeutics,* **139(1)**, 12(2013), **DOI:**10.1016/j.pharmthera.2013.03.002
8. H. K. Liu and P. J. Sadler, *Accounts of Chemical Research,* **44(5)**, 349(2011), **DOI:**10.1021/ar100140e
9. Y. Gilad and H. Senderowitz, *Journal of Chemical Information and Modeling,* **54(1)**, 96(2014), **DOI:**10.1021/ci400352t
10. R. H. Yu, Y. J. Zheng, Y. T. Li, Z. Y. Wu and C. W. Yan, *Transition Metal Chemistry,* **37(4)**, 399(2012), **DOI:**10.1007/s11243-012-9603-6
11. V. Prachayasittikul, S. Prachayasittikul, S. Ruchirawat and V. Prachayasittikul, *Drug Design, Development and Therapy*, **7**, 1157 (2013), **DOI:**10.2147/DDDT.S49763
12. M. Konagaya, A. Matsumoto, S. Takase, T. Mizutani, G. Sobue, T. Konishi, and Y. Matsuoka, *The Journal of the Neurological Sciences*, **218(1-2)**, 85(2004), **DOI:**10.1016/j.jns.2003.11.007
13. X. Hao, W. Chen, P. Zhan and X. Liu, *Medicinal Chemistry Communications,* **6(1)**, 61(2015), **DOI:**10.1039/C4MD00284A
14. Q. P. Qin, Z. F. Chen, J. L. Qin, X. J. He, Y. L. Li, Y. C. Liu and H. Liang, *European Journal of Medicinal Chemistry*,**92**, 302(2015), **DOI:**10.1016/j.ejmech.2014.12.052
15. K. P. Klugman and S.A. Madhi, *Infectious Disease Clinics of North America*, **13(3)**, 637(1999), **DOI:**10.1016/S0891-5520(05)70098-2
16. S. Apaydın M. Török, *Bioorganic & Medicinal Chemistry Letters*, **29(16)**, 2042(2019), **DOI:**10.1016/j.bmcl.2019.06.041
17. N. H. Bhuva, P. K. Talpara, P. M. Singala, V. K. Gothaliya and V. H. Shah, *Journal of Saudi Chemical Society*, **21(5)**, 517(2017), **DOI:**10.1016/j.jscs.2015.05.007
18. M. F. Hussein, *Mediterranean Journal of Chemistry*, **7(5)**, 370(2018), **DOI:**10.13171/mjc751912111445mh
19. H. J. Scholer, R. Leimer and R. Richle, *Antimalarial Drug II*, Springer, Berlin, Heidelberg, pp.123-206 (1984), **DOI:**10.1007/978-3-642-69254-3_4
20. S. L. Zaidi, S. M. Agarwal, P. Chavalitshewinkoon-Petmitr, T. Suksangpleng, K. Ahmad, F. Avecilla and A. Azam, *RSC Advances*, **6(93)**, 90371(2016), **DOI:**10.1039/C6RA15181G
21. J. Lin, D. C. Sahakian, S. M. De Morais, J. J. Xu, R. J. Polzer and S. M. Winter, *Current Topics in Medicinal Chemistry*, **3(10)**, 1125(2003), **DOI:**10.2174/1568026033452096
22. J. A. Jacobsen, J. L. Fullagar, M. T. Miller and S. M. Cohen, *Journal of Medicinal Chemistry***, 54(2)**, 591(2011), **DOI:**10.1021/jm101266s
23. S. A. Ibrahim, M. A. El-Gahami, R. M. Mahfouz, K. A. Farghali, *Z. Naturforsc B,* **44(12)**, 1488(1989), **DOI:**10.1515/znb-1989-1203
24. P. A. Wayne, *CLSI Document M27-A2* ((2002),
25. S. F. Vanparia, T. S. Patel, R. B. Dixit and B. C. Dixit, *Medicinal Chemistry Research***, 22(11)**, 5184(2013), **DOI:**10.1007/s00044-012-0320-7
26. Y. Liu, K. Zhang, R. Lei, J. Liu, T. Zhou and Z. Y. Yang, *Journal of Coordination Chemistry,* **65(12)**, 2041(2012), **DOI:**10.1080/00958972.2012.683485
27. M. N. Patel, M. R. Chhasatia and D. S. Gandhi, *Bioorganic & Medicinal Chemistry* Letters, **19(10)** 2870(2009), **DOI:**10.1016/j.bmcl.2009.03.078
28. T. Kondori, N. Akbarzadeh-T, K. Abdi, M. Dušek and V. Eigner, *Journal of Biomolecular Structure and Dynamics,* **38(1)**, 236(2020), **DOI:**10.1080/07391102.2019.1570867

29. E. M Zayed, M.M.H. Ahmed and G. G. Mohamed, *Applied Organometallic Chemistry*, **32(1)** 3952 (2018), **DOI:**10.1002/aoc.3952
30. L. Warren, "DeLano" The PyMOL Molecular Graphics System, *DeLano Scientific LLC, San Carlos.:‹ http://www. pymol. org* (2002),
31. BIOVIA, Dassault Systèmes. "Discovery studio visualizer." *San Diego, CA, USA,* (2017)
32. S. M. D. Rizvi, S. Shakil and M. Haneef, *EXCLI Journal*, **12**, 831(2013),
33. R. M. Silverstein and G. C. Bassler, *Journal of Chemical Education,* **39(11)**, 546(1962), **DOI:**10.1021/ed039p546
34. H. Nakamura, T. Yoshida, M. Todoko, K. Ueno and M. Takagi, *Bulletin of the Chemical Society of Japan*, **57(10)**, 2839(1984), **DOI:**10.1246/bcsj.57.2839
35. K. C. Satpathy, A. K. Panda, R. Mishra and I. Panda, *Synthesis and Reactivity in Inorganic and Metal-Organic Chemistry*, **21(4)**, 531(1991), **DOI:**10.1080/15533179108016823
36. G. J. Kharadi, J. R. Patel and B. Z. Dholakiya, *Applied Organometallic Chemistry***,** **24(11)**, 821(2010), **DOI:**10.1016/j.saa.2013.09.049
37. S. S. A. A. J. Abdul, S. R. Nasser and G. Brindha, *Chemical Science Transactions*, **3(1)**, 303(2014), **DOI:**10.7598/cst2014.641
38. R. M. Silverstein and G. C. Bassler, *Journal of Chemical Education,* **39(11)**, 546(1962), **DOI:**10.1021/ed039p546
39. H. L. Jing, H. P. Zeng, Y. D. Zhou, T. T. Wang, G. Z. Yuan and X. H. Ouyang, *Chinese Journal of Chemisry,* **24(7)**, 966(2006), **DOI:**10.1002/cjoc.200690183
40. a) G. Gliemann and A. B. P. Lever, Inorganic Electronic Spectroscopy, Studies in Physical and Theoretical Chemistry. Vol. 33 aus (1984). b) D. K. Swamy, S. P. Pachling and T. M. Bhagat. *Rasayan Journal of Chemistry*, **2(5)**, 208(2012)
41. A.V. Nikolaev, V. A. Logvinenko and L. I. Myachina, *In Thermal Analysis,* Academic Press, pp. 779-791 (1969), **DOI:**10.1081/SIM-120021646
42. R. B. Dixit, S. F. Vanparia, T. S. Patel, C. L. Jagani, H. V. Doshi and B. C. Dixit, *Applied Organometallic Chemistry***,** **24(5)**, 408(2010), **DOI:**10.1002/aoc.1631
43. A. Arslantas, A. K. Devrim, M. Sözmen, and H. Necefoglu, *Rasayan Journal of Chemistry*, **3(2)**, 201(2010)
44. G. Puthilibai, S. Vasudhevan, *Rasayan Journal of Chemistry*, **12(2)**, 855(2019)
45. T. Kondori, N. Akbarzadeh-T and C. Graiff, *Journal of the Iranian Chemical Society,* **16(9)**, 1827(2019), **DOI:**10.1007/s13738-019-01656-9
46. D. Santos-Martins, S. Forli, M. J. Ramos and A. J. Olson, *Journal of Chemical and Information Modeling,* **54(8)**, 2371(2014), **DOI:**10.1021/ci500209e
47. (a) I. Irfan, M. Irfan, M. Abid, and A. Azam, *Rasayan Journal of Chemistry*, **12(4)**, 2082(2019), **DOI:**10.31788/RJC.2019.1245320; (b) C. A. Lipinski, *Drug Discovery Today Technologies,* **1(4)**, 337(2004), **DOI:**10.1016/j.ddtec.2004.11.007
48. X. L. Ma, C. Chen and J. Yang, *Acta Pharmacologica Sinica,* **26(4)**, 500(2005), **DOI:**10.1111/j.1745-7254.2005.00068.x
49. S. Yamashita, T. Furubayashi, M. Kataoka, T. Sakane, H. Sezaki and H. Tokuda, *European Journal of Pharmamaceutical Science,* **10(3)**, 195(2000), **DOI:**10.1016/s0928-0987(00)00076-2

[RJC-5922/2020]